Assistive Technology Lab
3-59 Corbett Hall – University of Alberta Edmonton, AB T6G 2G4
Ph: (780) 492-5422 Fax: (780) 492-1696 Email: atlab@ualberta.ca

Published citation:
M. Najafi, K. Adams, and M. Tavakoli (2017, June). Robotic Learning from Demonstration of Therapist's Time-Varying Assistance to a Patient in Trajectory-Following Tasks. IEEE International Conference on Rehabilitation Robotics (ICORR) (In Press)

Robotic Learning From Demonstration of Therapist's Time-Varying Assistance to a Patient in Trajectory-Following Tasks

Mohammad Najafi, Kim Adams and Mahdi Tavakoli

***Abstract*—The number of people with physical disabilities and impaired motion control is increasing. Consequently, there is a growing demand for intelligent assistive robotic systems to cooperate with people with disability and help them carry out different tasks. To this end, our group has pioneered the use of robot learning from demonstration (RLfD) techniques, which eliminate the need for task-specific robot programming, in robotic rehabilitation and assistive technologies settings. First, in the demonstration phase, the therapist (or in general, a helper) provides an intervention (typically assistance) and cooperatively performs a task with a patient several times. The demonstrated motion is modelled by a statistical RLfD algorithm, which will later be used in the robot controllers to reproduce a similar intervention robotically. In this paper, by proposing a Tangential-Normal Varying-Impedance Controller (TNVIC), the robotic manipulator not only follows the therapist's demonstrated motion, but also mimics his/her interaction impedance during the therapeutic/assistive intervention. The feasibility and efficacy of the proposed framework are evaluated by conducting an experiment involving a healthy adult with cerebral palsy symptoms being induced using transcutaneous electrical nerve stimulation.**

I. Introduction

Loss of motor function, reduced mobility, restricted range of motion, muscle stiffness and inability to control the body movements are symptoms associated with a wide range of disorders including cerebral palsy (CP) and stroke, which are the most prevalent sources of severe disabilities in children and adults, respectively [1, 2]. In the upcoming years, population aging will further increase the number of affected people [3]. In the USA alone, there are 6.6 million stroke survivors, which is estimated to represent a burden of 33 billion dollars on the national health care system [4]. Also, more than 500,000 children under the age of 18 have at least one CP symptom that can interrupt their normal physical and social interaction [5, 6]. This sometimes results in incomplete cognitive and linguistic developments and imposes a heavy burden on economy, taking into consideration the long life expectancy for the affected children [7]. Due to the cost and labor intensity of conventional hand-over-hand rehabilitative and assistive practices, there has been a growing interest in robotic systems to take over some labor. Robotic systems are consistent, untiring and robust in repetitive task executions. Also, with the sensory data and cutting-edge artificial intelligent (AI), these systems can evaluate the patient's motor performance and accordingly provide the required assistance. In the near future, with the developments in AI and machine learning, assistive and rehabilitative robotic systems can become fully autonomous, making therapist's role of a supervisory nature. However, AI needs more development to be reliable for fully autonomous assistive robotic systems considering the complexity of certain tasks and the required safety guarantees in interaction with patients. Therefore, *semi-autonomous* Robot Learning from Demonstration (RLfD), which has originally been developed for service robotics and factory automation applications [8], is the focused in this paper. In this framework, only a short duration of the therapist's interaction with the patient (through a robotic medium) is enough to learn the task-specific assistance provided by the therapist to the patient and subsequently administer the same assistance to the patient robotically in the therapist's absence.

The RLfD is an intuitive technique for robot programming by physically demonstrating the intended task to a robotic manipulator. Assistive and rehabilitative systems are mainly used in therapeutic settings such as clinics and patients' homes, where computer and robot programming skills are not necessarily widely available. Recently in [9, 10], our group has suggested RLfD as an alternative for robot programming of assist-as-needed (AAN) rehabilitation systems. First, a therapist demonstrates the task to be done by the patient to the robotic manipulator for several times. Then, a Gaussian mixture model (GMM) models the

This research was supported by the Canada Foundation for Innovation (CFI) under grant LOF 28241, the Alberta Innovation and Advanced Education Ministry under Small Equipment Grant RCP-12-021, the Natural Sciences and Engineering Research Council (NSERC) of Canada under a Collaborative Health Research Projects (CHRP) Grant, Canadian Institutes of Health Research (CIHR), and the Quanser, Inc.

M. Najafi and M. Tavakoli are with the Departments of Electrical and Computer Engineering in University of Alberta, Edmonton, AB, Canada. (e-mail: najafi@ualberta.ca, mahdi.tavakoli@ualberta.ca).

K. Adams is with Faculty of Rehabilitation Medicine in University of Alberta, and Glenrose Rehabilitation Hospital, Edmonton, AB, Canada. (e-mail: kdadams@ualberta.ca).

demonstrated trajectories. Finally, in the reproduction phase, Gaussian mixture regression (GMR) produces a statistically desired trajectory from GMM, and a proportional-integral-derivative (PID) controller assists the patient, in the therapist's absence, to follow this desired trajectory.

In our previous work, we utilized impedance controllers to assist the patient around the desired trajectory learnt by the RLfD [11]. Two unvarying virtual impedance models attracted the patient's hand (which is holding the robot manipulator) to the desired trajectory, tangent and normal to the desired trajectory, providing him/her with an adjustable level of freedom in each direction. The more the patient deviates from the desired trajectory, the higher the attracting force towards the desired trajectory. This provided the patient with the experience of going through a virtual tunnel, with the patient having freedom along a tangential direction (along the tunnel) and a normal direction (sideways inside the tunnel). Since the width of the virtual tunnel was selected based on the narrowest section of the demonstrated trajectory, excessive assistance was provided in the rest of the path. To address this problem, in this paper, we propose a Tangential-Normal Varying Impedance Controller (TNVIC). Using the TNVIC, the level of assistance provided to the patient (related to the impedances imposed about the desired trajectory) changes in inverse proportion to the trial-to-trial variation in the demonstrated trajectories . Thus, the lower the variability in demonstrations at a given time, the more assistance is required to be provided to the patient, thus the higher the impedance parameters (spring-damper) to restrict deviation from the desired trajectory. This approach for impedance learning in the RLfD was proposed in [12] and also applied in [13] to learn human interaction impedance.

In this paper, the therapist and the patient cooperatively perform a given task for a few number of times, using a robotic manipulator. The therapist provides assistance such that the patient can complete the task, considering that more variability will result in less assistance to the patient (i.e., more freedom for the patient to deviate from the desired trajectory) in the reproduction phase. Then, using the GMM, the joint time-position data of demonstrated trajectories is captured statistically. Finally, in the therapist's absence, the GMR will extract the demonstrated average trajectory and also its trial-to-trial variability at each time from the GMM. The proposed TNVIC assists the patient to follow the average trajectory while imitating the therapist time-varying assistance based on the acquired variability (via impedance control) in tangential and normal directions (Fig. 1). Other features and novelties of this paper are:

- Unlike the previous RLfD frameworks for AAN [9, 10], where a varying PID controller was used to represent the variability observed in the demonstrations of the task, in the proposed TNVIC we use impedance controllers that have been widely utilized in human-robot interaction to regulate the interaction between the patient and the robotic manipulator.
- In TNVIC, the impedance models vary inversely proportional to the demonstrated trial-to-trial variability with consideration of the maximum interaction force (by the patient) to accurately assist the patient to remain in the demonstrated range of variability. However in [12, 13], linear and sigmoid functions were used to approximate the inverse relation of impedance parameters and variability.

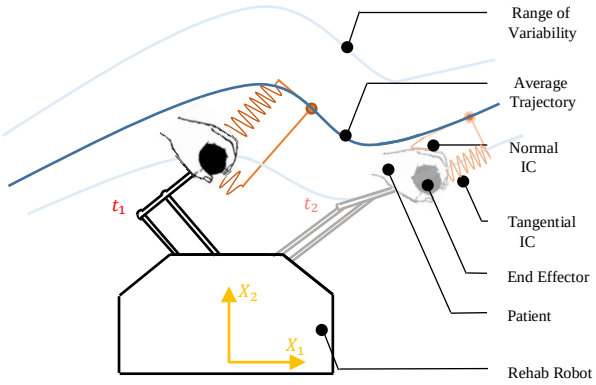

Fig. 1. In the demonstration phase, the therapist and the patient cooperatively perform the task for a number of trials. Then, using robot learning from demonstration, the task is modelled as an average trajectory (centroid of virtual tunnel) and variations in trajectory (width of the virtual tunnel). The proposed TNVIC assists the patient by two varying impedance models (spring-damper) to follow the demonstrated trajectory and remain in the demonstrated range of variability. This figure shows the TNVIC in two time instances (t_1, t_2). The less the variability, the higher (the more stiff) the impedance models in tangential and normal directions to allow lower deviations by the patient about the average trajectory.

II. Cooperative Task Demonstration

Reaching motions are routinely part of rehabilitation exercises. For simplicity, the task is constrained to a 2-dimensional Cartesian space. It is assumed that the patient is unable to complete a given task, if unassisted. Therefore, the therapist also interacts with the robotic manipulator held by the patient in order to assist the patient to carry out the task, considering the patient's constraints and range of motion. A few cooperative task trials is sufficient to demonstrate to the robotic manipulator the required assistance.

A. Data sampling and arrangement

During the demonstration phase, the 2-dimensional position signal in the Cartesian coordinates ($\xi_P \in R^2$) and the time variable ($\xi_t \in R$) are sampled and jointly denoted as ξ. Having M task demonstrations (i.e., trials), respectively consisting of $\{N^j,\ \mathrm{j} = 1, \dots, \mathrm{M}\}$ samples, the entire demonstrated data can be organized as

$$D = \left\{\{\xi^{i,j}\}_{i=1}^{N^j}\right\}_{j=1}^{M},\quad \forall\, \xi^{i,j} = \begin{bmatrix}\xi_P^{i,j}\\ \xi_t^{i,j}\end{bmatrix} \in R^3, \tag{1}$$

where $\xi^{i,j}$ represents the i^{th} sample of the j^{th} demonstration. The data (D) consists of $\sum_{j=1}^{M} N^j$ discrete samples.

B. Gaussian Mixture Model (GMM)

The GMM statistically models the demonstrated data by a sum of weighted Gaussians [8]. A Gaussian probability

density function (PDF), also known as the normal distribution, has been widely used to model physical phenomenon such as human movements. A single Gaussian PDF is unable to capture inevitable nonlinearities in the complex trajectory-following tasks. Hence, the GMM uses a mixture of K individual Gaussians as shown in Fig. 2. The

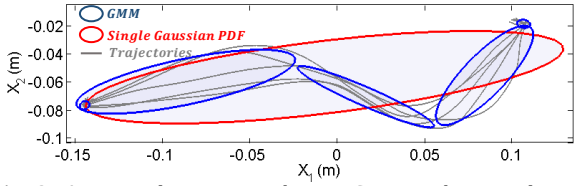

Fig. 2. An example scenario where a GMM with its 5 clusters (Blue ellipsoids) captures the nonlinearities in demonstrated trajectories, as compared to a Single Gaussian PDF (Red ellipsoid). Note that this figure displays the reflection of the 3-dimensional trajectories and GMM over the 2-dimensional spatial axes.

GMM as a PDF operator (f) that models the demonstrated data (D) with its variable ξ is expressed as

$$f(\xi|\theta^i) = \sum_{i=1}^{K} \pi^i \mathcal{N}_3(\xi|\mu^i, \Sigma^i), \quad (2)$$
$$\forall\, 0 < \pi^i < 1 \;\&\; \sum_{i=1}^{K} \pi^i = 1 \;\&\; \Sigma^i = \begin{bmatrix} \Sigma_p^i & \Sigma_{p,t}^i \\ \Sigma_{t,p}^i & \Sigma_t^i \end{bmatrix} > 0,$$

where $\theta^i = \{\pi^i \in R^3, \mu^i \in R^3, \Sigma^i \in R^{3\times3}\}_{i=1}^{K}$ are made up of parameters of the GMM, i.e., the prior weight, the mean and the covariance matrix for each of the K Gaussian components, respectively. $\mathcal{N}_n$ denotes the n-dimensional Normal PDF (Appendix I). The optimum number of components (K) is chosen, using Bayesian Information Criterion, which penalize the complexity of the GMM model [14]. The GMM parameters ($\{\theta^i\}_{i=1}^{K}$) are learned, using Expectation Maximization algorithm [15].

Now, all the discrete $\sum_{j=1}^{M} N^j$ samples, each consisting of a position variable ($\xi_p \in R^2$) and a time variable ($\xi_t \in R$), are modeled by the sum of K weighted Gaussian PDFs which capture the demonstrated trajectories in terms of its average and its variations in the position-time space.

III. ROBOTIC SEMI-AUTONOMOUS ASSISTANCE

In this section, the aim is to provide a framework to robotically reproduce the assistance provided by the therapist in order to assist the patient in completing the task in the therapist's absence. For this purpose, at each time, the expected position captured by GMM is extracted via GMR. Then, using the proposed TNVIC, the user is assisted to reach this expected (desired) position, mimicking the therapist intervention by considering the demonstrated trial-to-trial variability in tangential and normal directions.

A. Gaussian Mixture Regression (GMR)

Extracting data from the learned 3-dimensional GMM in Section II, and feeding it to the robot controller in real-time requires a regression technique to approximate the expected (desired) 2-dimensional position (ξ_P) in a given time ($\xi_t = t$). In this paper, GMR is used as a probabilistic operator that approximates a single Gaussian PDF of the expected position (ξ_P) by calculating a conditional probability on the learnt GMM [9], as (3), in which $\widehat{\mu_{P,t}} \in R^2$ and $\widehat{\Sigma_{P,t}} \in R^{2\times2}$ approximate the average and covariance matrices of the demonstrated position at a given time $\xi_t = t$. (Fig. 3).

$$f(\xi_P|\xi_t = t) \approx \mathcal{N}_2\left(\xi_P\middle|\widehat{\mu_{P,t}}, \widehat{\Sigma_{P,t}}\right), \quad (3)$$

B. Tangential-Normal Varying Impedance Controller (TNVIC)

The TNVIC assists the patient to follow the average demonstrated trajectory ($\widehat{\mu_{P,t}}$) using two time-varying virtual spring-damper impedance models. In real-time, $\widehat{\mu_{P,t}}$ acts as a target moving along the average demonstrated trajectory. The impedance models (spring-damper) virtually connect the robot end-effector (held by the patient) to the moving target ($\widehat{\mu_{P,t}}$), respectively in tangential and normal coordinate system (*T-N*), as

$$c_{T,t}\dot{\widetilde{\xi_{P_T}}} + k_{T,t}\widetilde{\xi_{P_T}} = -F_{P_T}, \quad (4)$$
$$c_{N,t}\dot{\widetilde{\xi_{P_N}}} + k_{N,t}\widetilde{\xi_{P_N}} = -F_{P_N}, \quad (5)$$

where $\{c_{T,t}, k_{T,t}\} \in R^+$ and $\{c_{N,t}, k_{N,t}\} \in R^+$ denote the desired time-varying damping and stiffness in *T-N*. $\widetilde{\xi_{P_T}}$ and $\widetilde{\xi_{P_N}}$ indicate the deviation with respect to $\widehat{\mu_{P,t}}$, resulting from the patient's force exertions in tangential (F_{P_T}) and normal (F_{P_N}) directions.

The *direction* and *magnitude* of the two orthogonal impedance models vary based on the demonstrated average ($\widehat{\mu_{P,t}}$) and variability ($\widehat{\Sigma_{P,t}}$) as follows.

Direction: The impedance controllers rotate to be tangent/normal to the average demonstrated trajectory. The *T-N* at a given time (t) is centered on the desired trajectory $\widehat{\mu_{P,t}}$ and rotated with respect to an inertial Cartesian coordinate system X_1-X_2 with angle

$$\theta_{R,t} = \arctan\left(\left(\widehat{\mu_{p_{X_2},t}} - \mu_{\widehat{p_{X_2},t-T}}\right)/\left(\widehat{\mu_{p_{X_1},t}} - \mu_{\widehat{p_{X_1},t-T}}\right)\right) \quad (6)$$

where $\widehat{\mu_{p_{X_2},t}}$ and $\widehat{\mu_{p_{X_1},t}}$ represent the projection of $\widehat{\mu_{P,t}}$ on X_1-X_2. T denotes the sampling period. Therefore the rotation matrix from X_1-X_2 to *T-N* is

$$R_{R,t} = \begin{bmatrix} cos(\theta_{R,t}) & sin(\theta_{R,t}) \\ -sin(\theta_{R,t}) & cos(\theta_{R,t}) \end{bmatrix}. \quad (7)$$

Magnitude: The impedance parameters are in inverse proportion relation to the variability of the demonstrated trajectories. Following Hooke's law, with a constant force exerted by the patient on a spring that connects the robotic manipulator to the desired trajectory, the resulted deviation is inversely proportional to the spring magnitude (stiffness) as $\widetilde{\xi_P} = F_a / k$. Therefore, to mimic the therapist's assistance (i.e., the therapist variable interaction stiffness),

the spring magnitudes are selected inversely proportional to the demonstrated variability (as shown in Fig. 4) in each of tangential and normal direction so that the patient can not deviate more than the demonstrated range of variability

$$\{k_{\varsigma,t} = F_{P,max}/3\sigma_{\varsigma,t}\,; \quad if\ (k_{\varsigma,t} > k_{max}) \rightarrow k_{\varsigma,t} = k_{max}\}, \tag{8}$$

where $\varsigma = \{T, N\}$, should be substituted with T *or* N syntaxes to represent the equation for variable spring value in tangent-

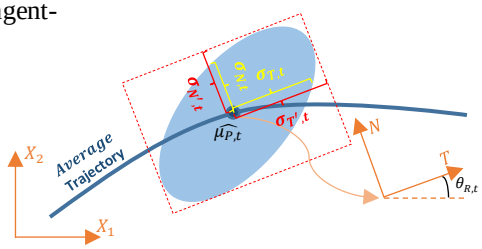

Fig. 3. The calculation of standard deviation in tangential and normal directions, using (9) and (10).

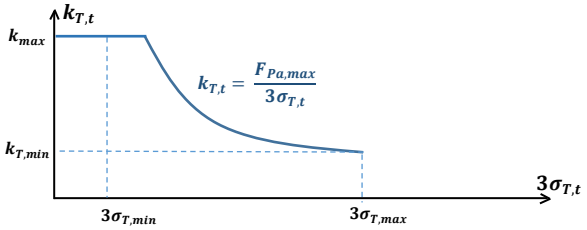

Fig. 4. The inverse proportional relationship between stiffness and standard deviation in tangential direction when $k_{T,max}$ ($k_{T,t}$ when $\sigma_{T,t} = \sigma_{T,min}$) is larger than k_{max}.

ial *or* normal directions, respectively. k_{max} is the maximum stiffness determined by the user for hardware restriction. $\sigma_{\varsigma,t}$ denotes the demonstrated standard deviation along tangential ($\sigma_{T,t}$) or normal ($\sigma_{N,t}$) axis, which are extracted from rotated covariance matrix ($\widehat{\Sigma_{P_{T-N},t}}$) at each time, calculated from (9) and (10). $3\sigma_{\varsigma,t}$ is the distance to the average in Gaussian PDF that contains 99% of demonstrated trajectories. $F_{P,max}$, is the patient's maximum force, measured (or tuned) before robotic assistance.

$$\widehat{\Sigma_{P_{T-N},t}} = \begin{bmatrix} {\sigma_{T',t}}^2 & \rho_t \sigma_{T',t}\sigma_{N',t} \\ \rho_t \sigma_{T',t}\sigma_{N',t} & {\sigma_{N',t}}^2 \end{bmatrix} = R_{R,t}\, \widehat{\Sigma_{P,t}}\, {R_{R,t}}^T, \tag{9}$$

$$\sigma_{\varsigma,t} = \sqrt{1-{\rho_t}^2}.\sigma_{\varsigma',t}\ , \qquad \text{with} \qquad \varsigma = \{T, N\}, \tag{10}$$

$$c_{\varsigma,t} = \tau_\varsigma\, k_{\varsigma,t}\ ,\ \varsigma = \{T, N\}. \tag{11}$$

In (9) and (10), $\sigma_{N',t}$ and $\sigma_{T',t}$ represent the reflected standard deviation in *T-N* axes as shown in Fig. 3, ρ_t is the correlation factor, which is a constant value between zero and one. To adjust the transient response of the second-order impedance model, the damping ratio (τ_ς) is set to a constant value by calculating the damper parameter as (11). Finally, having the variable impedance models, and interaction force of patient (F_{Pa_T}, F_{Pa_N}), the resulting deviation ($\widetilde{\xi_{P_T}}, \widetilde{\xi_{P_N}}$), can be calculated from (4) and (5). The desired position ($\xi_{P,des}$) of the robotic manipulator followed by the PID position controller is the sum of the average demonstrated trajectory and patient deviation which are rotated back from *T-N* to X_1-X_2 as:

$$\begin{bmatrix} \xi_{P_{X_1},des} \\ \xi_{P_{X_2},des} \end{bmatrix} = \begin{bmatrix} \widehat{\mu_{P_{X_1},t}} \\ \widehat{\mu_{P_{X_2},t}} \end{bmatrix} + (R_{R,t})^{-1} \begin{bmatrix} \widetilde{\xi_{P_T}} \\ \widetilde{\xi_{P_N}} \end{bmatrix}. \tag{12}$$

The proposed TNVIC have been rigorously analyzed in Fig. 5 and Algorithm I.

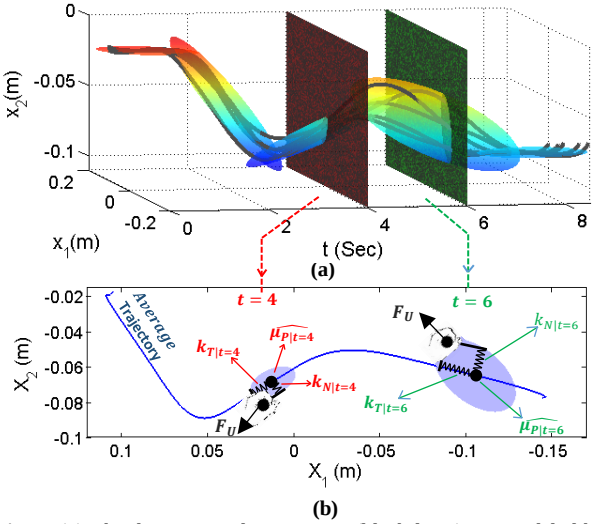

Fig. 5. (a) The demonstrated trajectories (black lines) are modeled by a 3-dimensional GMM (ellipsoids) in joint position-time space (Section II. B). The planes normal to the time axis (t), represent the Gaussian Mixture Regression. The expected demonstrated position in a given time is calculated by approximating a single 2-dimensional Gaussian PDF from the intersected mixture models (Section III.A). The times t = 4 and t = 6 are selected randomly to provide an example of the proposed robotic assist-as-needed framework. **(b)** Shows the proposed controller in (t = 4, t = 6).

Algorithm I: Tangential-Normal Varying Impedance Controller (TNVIC)

Initial Inputs: GMM model $\{\theta^i\}_{i=1}^K$. Patient's maximum force ($F_{p,max}$). Transient damping ratio (τ_ς), maximum stiffness ($K_{\max}$), and t = 0.

For t = t + T & t < max (demonstrated ξ_t)

Inputs: $\{F_{P_{X_1}}, F_{P_{X_2}}\}$, the patient's interaction force from force sensor

1: Extract the demonstrated average and variability in X_1-X_2 $\{\widehat{\mu_{P,t}}, \widehat{\Sigma_{P,t}}\}$,from the GMM, using the GMR by **(3).**

2: Calculate the TNVIC direction ($\theta_{R,t}$) from $\widehat{\mu_{P,t}}$ by **(6)**

3: Form the rotation matrix ($R_{R,t}$) from $\theta_{R,t}$ by **(7)**

4: Find the standard deviation in tangential and normal directions $\{\sigma_{\varsigma,t}\}$ from $\widehat{\Sigma_{P,t}}$, using $R_{R,t}$ by **(9)** and **(10).**

5: Map force sensor signal from X_1-X_2 to *T-N* using $R_{R,t}$.

6: Calculate the variable spring parameters ($k_{\varsigma,t}$), which is inversely proportional to $\sigma_{\varsigma|t}$ by **(8).**

7: Determine the variable damper parameters ($c_{\varsigma,t}$), from $\{k_{\varsigma,t}, \tau_\varsigma\}$ by **(11).**

8: Find the deviation ($\widetilde{\xi_{P_T}}, \widetilde{\xi_{P_N}}$), by solving the variable impedance controller, having the $\{c_{\varsigma,t}, k_{\varsigma,t}, F_P\}$ by **(4)** and **(5)**.

9: Calculate the desired position in X_1-X_2 ($\xi_{P,des}$) to be followed by the robotic manipulator, having the $\{\widehat{\mu_{P,t}}, \widetilde{\xi_{P_T}}, \widetilde{\xi_{P_N}}, R_{R,t}\}$.

Outputs: $\{\xi_{P_{X_1},des}, \xi_{P_{X_2},des}\}$**,** the desired position for robot end effector

IV. Experimental Validation and Discussion

The proposed framework is experimentally evaluated using a Quanser rehabilitation robot and implemented in QUARC real-time software (Quanser Consulting Inc., Markham, Canada) with a sampling frequency of 1 kHz. Without loss of generality, an application for assisting children with CP has been considered in this paper. Playing is vital for children's physical and mental cognitive development [5]. Nowadays, one of the common activities of children is using apps on smartphones, tablets and touchscreens. In order to help children with CP to also have the same experience, the proposed framework can be used to assist them in tasks, which can be represented by point-to-point motion primitives.

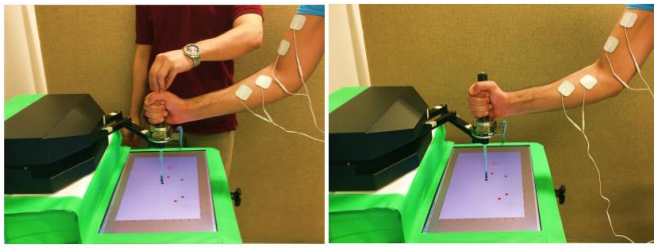

Fig. 6. This figure shows the experiment setup in both demonstration (Left) and robotic assistance (right) phases. Two pairs of transcutaneous electrical nerve stimulation pads were used for simulation of CP symptoms (Section.IV).

Table I. The selected system parameters

$\tau_\varsigma = .15\ sec$	$F_{P,max} = 10\ N$	$K_{max} = 1800\ N/m$

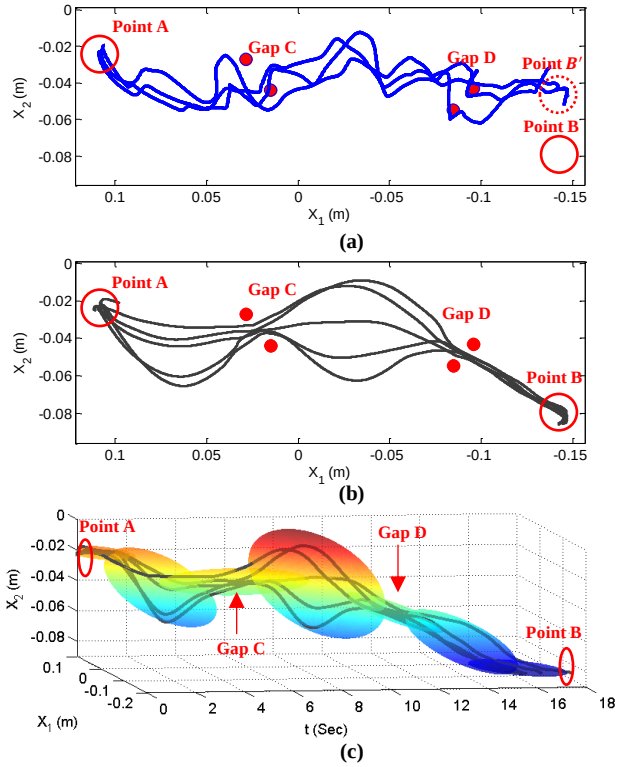

Fig. 7. (a) The patient trajectories in 3 consecutive trials. Point B' is projected on the LCD monitor instead of the actual destination (point B) to simulate poor coordination in patients with CP **(b)** The cooperative demonstration of therapist and patient for 5 trials. The therapist intentionally demonstrated more variability in sections where less assistance (accuracy) were required. Also, as the patient has difficulty to coordinate his movements from gap D to point B, the therapist provided less variability in this section. **(c)** This graphic displays the 3-dimensional GMM with its seven Gaussian mixtures (colored ellipsoids) that modeled the position-time joint trajectories of the therapist demonstration (black lines) with its average and variability.

A designed 2-dimensional virtual game was projected on an LCD screen placed under the robotic end effector as shown in Fig. 6. The user is expected to move the robotic end-effector (in contact with the LCD) from point A to point B, through two gaps with different directions and widths, as Fig. 7.

A. Simulation of cerebral palsy (CP) symptoms in healthy adults

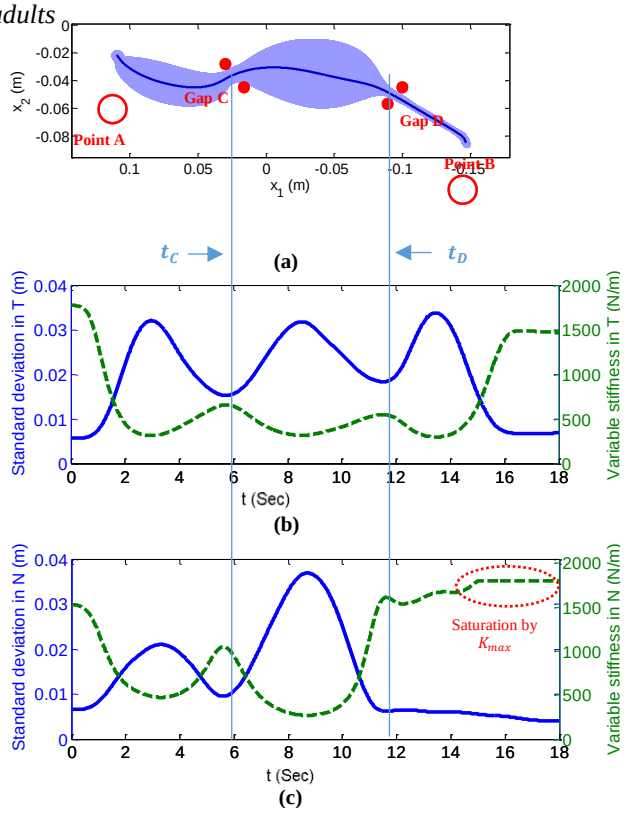

Fig. 8. (a) This figure demonstrates the expected position probability density function (PDF) approximated by GMR from the GMM (Fig. 7(c)) at all time samples in the robotic assistance. Note that in Fig. 5(b), the GMR results have been shown just in two time instances. The dark blue dots and blue area display the average and variability for 2-dimensional Gaussians PDFs in all time samples, respectively. **(b)** At each time, the standard deviation in tangential (T) direction (Blue plot) is extracted from the 2 dimensional PDF approximated by GMR. The tangential variable spring value (Stiffness) changes with inverse correlation to the standard deviation (8) to assist the patient to remain in the demonstrated range of variability (3×standard deviation) in each time sample. **(c)** Same as (b), but in normal (N) direction.

The main symptoms of CP are stiffness of muscles, limited range of motion, poor coordination, difficulties performing a
voluntary movement, weakness and tremor [5]. In this paper, to induce some of these symptoms in an adult without disability, transcutaneous electrical nerve stimulation (TENS) was employed. Low frequency stimulation of upper

arm muscles (biceps) and wrist muscles (Flexor carpi, Palmaris lunges, etc.), was chosen to provide the maximum correlation with the behavior observed in an actual CP patient [16]. Also, in order to make the situation more challenging for the system, point B' was projected on the LCD instead of the actual destination (point B) to represent the poor coordination (inability to accurately reach the destination) in patients with CP. The adult user in the presence of stimulation (called patient) was asked to perform the designed task and move from point A to point B, while passing through the Gap C and D without hitting them. As it is shown in Fig. 7(a), the user was unable to correctly accomplish this task without therapist assistance.

B. Demonstration

During the demonstration, a therapist intervene the task and provides the minimum required assistance. Considering the inverse correlation of the TNVIC assistance with the variability in the demonstrated trajectories, the therapist intentionally produce more variability between trials in regions where less assistance is required and vice versa (Fig. 8(b)). The cooperative task trajectories (5 trials) are then captured by the GMM to statistically model the task with its features (average and variability) as shown in Fig. 8(c).

C. Robotic semi-autonomous assistance

Using the proposed TNVIC, and system parameters in Table I, the robotic system imitates the therapist's time-varying intervention in the demonstration phase and assists the patient to complete the task successfully (Fig. 6). The desired position data calculated via GMR from GMM, and varying tangential and normal stiffness (spring parameter magnitude) are shown in Fig. 8. In this figure, t_C and t_D are associated with time instances that the average trajectory is in Gap C and Gap D, respectively. The patient is connected to the average trajectory with two virtual impedance models that regulate the level of assistance (stiffness) in each of tangential and normal directions. In Gap C and Gap D, due to the required accuracy, the therapist demonstrated low variability across trials. Therefore, it is expected to have high level of assistance accordingly. As observed in Fig. 8(b), at t_C and t_D, the variability (standard deviation) in tangential direction is lower from the adjacent time, therefore the variable tangential spring is stiffer to provide more assistance. This is due to the fact that in demonstration, therapist intuitively moved slower through sections where more accuracy was required. Same characteristic can be observed in Normal direction as displayed in Fig. 8(c). In gap C and gap D, the width of the path is narrower, thus more assistance is required in normal direction, accordingly. As Gap D is narrower than gap C, the therapist demonstrated less variability in Gap D. Therefore the normal stiffness (assistance) is higher in t_D than in t_C.

Using TNVIC, with its time-varying impedance models, the patient was assisted to perform the demonstrated task in contact with the robotic manipulator. Again, the point B', was projected on the LCD as the destination phase, to test if the system can assist the patient to reach the actual destination (point B). Fig. 9(a), displays that the patient successfully completed the task and moved from point A to point B, through gaps without hitting them. Fig. 9(b), shows the interaction force of the patient in normal direction. After Gap D, towards the destination (Point B), the patient exerted his maximum force to reach point B' (which he thinks is the destination). The controller successfully restricted the patient movement and dragged (assisted) his hand to the actual destination (point B). Between $t_{p,C}$ and $t_{p,D}$ ($t_{p,C}$ and $t_{p,D}$ are associate with approximate time instances that the patient passed gap C and gap D, respectively), the stiffness parameters were lowest in both tangential and normal directions (Fig. 8). Therefore, there was higher freedom for the patient to deviate. This extra freedom gave the patient the motivation to participate in the task and increase his force exertion which resulted in increased velocity variations (Fig. 9(c)). That is the cause for larger variations observed between $t_{p,C}$ and $t_{p,D}$, compared to t < $t_{p,C}$. The advantage of the proposed framework is to provide maximum possible freedom to the pa-

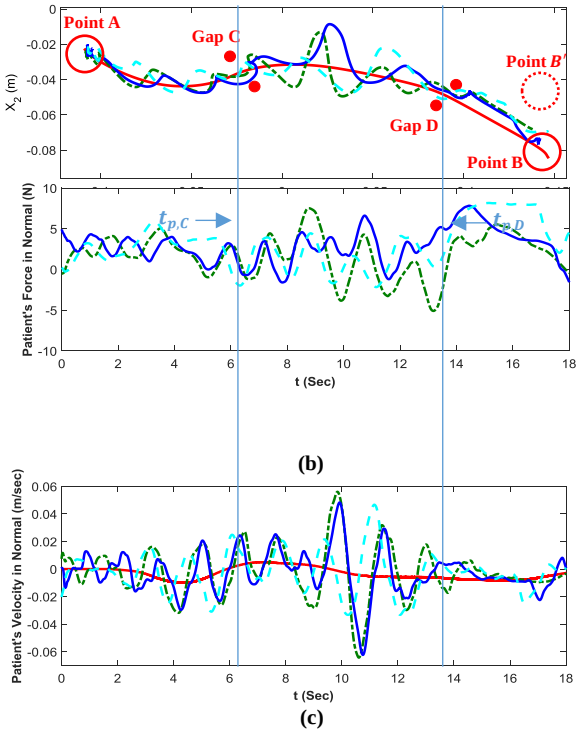

Fig. 9. **(a)** Displays the patient's trajectories in three consecutive task trials, being assisted by the robotic manipulator. The proposed TNVIC effectively assisted the patient to complete the task successfully.(The red plot is the average demonstrated trajectory) **(b)** Shows the patients interaction force with the robotic manipulator in normal direction. **(c)** Demonstrates the patient velocity in normal direction.

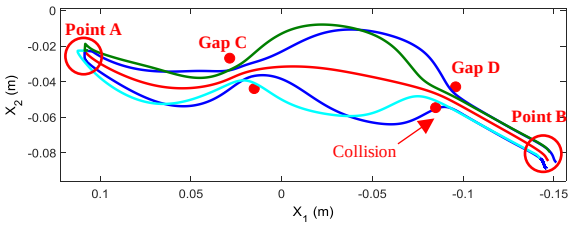

Fig. 10. The performance of system when the user's maximum force (10 N) is exerted on the system in 4 directions. $\{(F_{Pa_T}, F_{Pa_N})\}$ = {(7.14, 7.14), (7.14, -7.14), (-7.14, 7.14), (-7.14, -7.14); all in Newton (N) }. Note that as tangential normal directions are orthogonal, the projection of 10 N on each axis through Pythagorean law is 7.14 N.

tient (assist-as-needed) to motivate him/her for participation in task execution.

In TNVIC, the variable impedance parameters were adjusted to restrict the patient from deviating out of the expected position along tangential and normal directions, even if they exert their maximum interaction force. Therefore, any force exertion less than the measured (or tuned) maximum force, will end up in successful task completion, regardless of its direction and frequency. In Fig. 10, the robotic system was introduced with the patient's maximum force in 4 different directions (this values are assigned in the real-time controller) to observe the performance under some worst-case scenarios. As it is observed, just in one of the trials ($F_{Pa_T} = 7.14$ N, $F_{Pa_N} = -7.14$ N) there was a collision with Gap D. The possible source of this error are : 1) The robot position controller (PID). 2) The sudden increase in impedance parameters, before entering the Gap D (Fig. 8(c)). The impedance model is a dynamic system with tunable transient damping ratio (τ_ζ), so it cannot keep up accurately with sudden changes in the desired trajectory. These constraints can be considered by possibly adding a penalty factor to (8). In this experiments, a single trajectory-following task was successfully tested, however, the proposed framework is able to model complex trajectories as it uses GMM/GMR technique to model and reproduce tasks through time-indexing. Also, sequential tasks can be learnt and reproduced by several point-to-point motion primitives, discussed in this paper. Furthermore, using GMM/GMR, only few demonstrations are required to capture the trajectory smoothly and effectively as opposed to simply averaging the demonstrated trajectories. Also, the GMM captures the variability of trials and statistical correlation of task variables which are utilized in this paper to learn the therapist intended interaction impedance. The interaction impedance is actively controlled in robotic assistance phase, inversely proportion- al to the variability across trials in the demonstration phase to reproduce the intended time-varying impedance of the therapist.

All in all, the proposed framework has merits in rehabilitation and assistive technologies to replicate the therapist short intervention (usually assistance) in trajectory-following tasks that have to be repeated several times. In the future, the main focus of our work will be to: 1) extend the proposed framework to generalize the therapist demonstrated assistance for tasks with varying parameters (e.g. the location, direction, or width of the gaps in this paper). Currently, the proposed framework is task-specific and requires new demonstrations by the therapist if any of the parameters change. 2) Add an adaptive law to the proposed controller to adapt to the performance of the patient during the robotic assistance phase. The proposed TNVIC is non-adaptive, in the sense that the controller provide same assistance (as-demonstrated), even if the patient behaves different from the demonstration phase (e.g. gets tired or enhances his performance by repetition).

V. Conclusion

While, the proposed semi-autonomous robotic assistance framework can have a plethora of applications in cooperative human-robot task execution, without the loss of generality, a potential application in assist-as-needed rehabilitation for tasks with trajectory-following characteristic was discussed in this paper. The framework, with its robot learning from demonstration (RLfD) framework and tangential-normal varying-impedance controller (TNVIC) were developed precisely in this paper. The efficacy and performance of the system was evaluated in demonstration, RLfD, and semi-autonomous robotic assistance phases, with an healthy adult induced with CP symptoms, using Transcutaneous electrical nerve stimulation. Also, the limitations of the proposed framework, and future focus for finding the possible solutions have been discussed.

Appendix I

The n-dimensional normal probability density function with its average μ and covariance matrix Σ is:

$$\mathcal{N}_n(\xi|\mu,\Sigma) = \frac{1}{\sqrt{(2\pi)^n|\Sigma|}}\, e^{-\frac{1}{2}\left((\xi-\mu)^T\Sigma^{-1}((\xi-\mu))\right)};$$

$$\forall\, \mu, \xi \in R^n, \qquad \Sigma \in R^{n\times n}$$

References

[1] N. Paneth, T. Hong, and S. Korzeniewski, "The Descriptive Epidemiology of Cerebral Palsy," *Clinics in Perinatology*, vol. 33, pp. 251-267, 2006.

[2] J. Adamson, A. Beswick, and S. Ebrahim, "Is stroke the most common cause of disability?," *Journal of Stroke and Cerebrovascular Diseases*, vol. 13, pp. 171-177, 2004.

[3] H. P. van der Ploeg, A. J. van der Beek, L. H. van der Woude, and W. van Mechelen, "Physical Activity for People with a Disability," *Sports Medicine*, vol. 34, pp. 639-649, 2004.

[4] D. Mozaffarian, E. J. Benjamin, A. S. Go, D. K. Arnett, M. J. Blaha, M. Cushman, *et al.*, "Executive Summary: Heart Disease and Stroke Statistics," *Circulation*, vol. 133, p. 447, 2016.

[5] A. Johnson, "Prevalence and characteristics of children with cerebral palsy in Europe," *Developmental Medicine and Child Neurology*, p. 7, 2002.

[6] A. M. Ríos-Rincón, K. Adams, J. Magill-Evans, and A. Cook, "Playfulness in Children with Limited Motor Abilities When Using a Robot," *Physical & Occupational Therapy In Pediatrics*, vol. 36, pp. 232-246, 2016/07/02 2016.

[7] T. Klein, G. J. Gelderblom, L. d. Witte, and S. Vanstipelen, "Evaluation of short term effects of the IROMEC robotic toy for children with developmental disabilities," *IEEE International Conference on Rehabilitation Robotics*, 2011, pp. 1-5.

[8] Sonia Chernova; Andrea L. Thomaz, "Robot Learning from Human Teachers," *Robot Learning from Human Teachers* ,1, Morgan & Claypool, 2014, pp.121-

[9] M. Maaref, A. Rezazadeh, K. Shamaei, and M. Tavakoli, "A Gaussian Mixture Framework for Co-Operative Rehabilitation Therapy in Assistive Impedance-Based Tasks," *IEEE Journal of Selected Topics in Signal Processing*, vol. 10, pp. 904-913, 2016.

[10] M. Maaref, A. Rezazadeh, K. Shamaei, R. Ocampo, and M. Tavakoli, "A Bicycle Cranking Model for Assist-as-Needed Robotic Rehabilitation Therapy Using Learning From Demonstration," *IEEE Robotics and Automation Letters*, vol. 1, pp. 653-660, 2016.

[11] M. Najafi, M. Sharifi, K. Adams, and M. Tavakoli, "Robotic assistance for children with cerebral palsy based on learning from tele-cooperative demonstration," *International Journal of Intelligent Robotics and Applications*, pp. 1-12, 2017.

[12] S. Calinon, I. Sardellitti, and D. G. Caldwell, "Learning-based control strategy for safe human-robot interaction exploiting task and robot redundancies," in *2010 IEEE/RSJ International Conference on Intelligent Robots and Systems*, 2010, pp. 249-254.

[13] M. Saveriano and D. Lee, "Learning motion and impedance behaviors from human demonstrations," in *2014 11th International Conference on Ubiquitous Robots and Ambient Intelligence (URAI)*, 2014, pp. 368-373.

[14] G. Schwarz, "Estimating the dimension of a model," *Annals of Statistics*, vol. 6, pp. 461-464, 1978.

[15] T. K. Moon, "The expectation-maximization algorithm," *IEEE Signal Processing Magazine*, vol. 13, pp. 47-60, 1996.

[16] I. Sakamaki, M. Gomez, J. Castanellos , M. Tavakoli, N. Jafari, K. Adams,"Design and preliminary testing of a haptics-assisted robot platform for play by children with physical impairments," *Journal of Assistive Technology*, 2016.